

Steady-State and Stopped-Flow Kinetic Studies of Three *Escherichia coli* NfsB Mutants with Enhanced Activity for the Prodrug CB1954[†]

David Jarrom,^{‡,⊥,‡} Mansooreh Jaberipour,^{§,⊥,Δ} Christopher P. Guise,^{§,▽} Simon Daff,^{||} Scott A. White,[‡] Peter F. Searle,[§] and Eva I. Hyde^{*,‡}

[‡]School of Biosciences and [§]Institute for Cancer Studies, The University of Birmingham, Edgbaston, Birmingham B15 2TT, U.K., and ^{||}School of Chemistry, University of Edinburgh, Joseph Black Building, West Mains Road, Edinburgh EH9 3JJ, U.K. [⊥]D.J. and M.J. contributed equally to this study (joint first authors). [‡]Current address: Current Biodata Ltd., Swansea SA1 8PH, U.K. ^ΔCurrent address: Institute for Cancer Research, Shiraz University of Medical Sciences, Zand St., Shiraz, Iran 71345-3119. [▽]Current address: Auckland Cancer Society Research Centre, The University of Auckland, Private Bag 92019, Auckland, New Zealand.

Received April 20, 2009; Revised Manuscript Received July 4, 2009

ABSTRACT: The enzyme nitroreductase, NfsB, from *Escherichia coli* has entered clinical trials for cancer gene therapy with the prodrug CB1954 [5-(aziridin-1-yl)-2,4-dinitrobenzamide]. However, CB1954 is a poor substrate for the enzyme. Previously we made several NfsB mutants that show better activity with CB1954 in a cell-killing assay in *E. coli*. Here we compare the kinetic parameters of wild-type NfsB with CB1954 to those of the most active single, double, and triple mutants isolated to date. For wild-type NfsB the global kinetic parameters for both k_{cat} and K_{m} for CB1954 are about 20-fold higher than previously estimated; however, the measured specificity constant, $k_{\text{cat}}/K_{\text{m}}$ is the same. All of the mutants are more active with CB1954 than the wild-type enzyme, the most active mutant showing about 100-fold improved specificity constant with CB1954 over the wild-type protein with little effect on k_{cat} . This enhancement in specificity constants for the mutants is not seen with the antibiotic nitrofurazone as substrate, leading to reversed nitroaromatic substrate selectivity for the double and triple mutants. However, similar enhancements in specificity constants are found with the quinone menadione. Stopped-flow kinetic studies suggest that the rate-determining step of the reaction is likely to be the release of products. The most active mutant is also selective for the 4-nitro group of CB1954, rather than the 2-nitro group, giving the more cytotoxic reduction product. The double and triple mutants should be much more effective enzymes for use with CB1954 in prodrug-activation gene therapy.

Nitroreductases are NAD(P)H-dependent flavoproteins found in many bacteria that catalyze the reduction of a wide range of aromatic nitro compounds (Scheme 1; reviewed in ref 1). They have been proposed for use in bioremediation of toxic products from industrial processes such as manufacture of explosives, for biocatalysis for synthesis of dyestuffs and pesticides, and for cell ablation. The NfsB enzyme from *Escherichia coli* has been in clinical trials for use in cancer gene therapy in combination with the prodrug CB1954¹ [5-(aziridin-1-yl)-2,4-dinitrobenzamide] (2, 3). NfsB catalyzes the reduction of either (but not both) of the two nitro groups of CB1954 in equal proportions to the corresponding hydroxylamine derivatives. The 4-hydroxylamine derivative of the prodrug is further activated *in vivo* and generates interstrand DNA cross-links (4). These cross-links are poorly repaired and cause cell death in both dividing and nondividing cells. Human cells are normally resistant to the prodrug, but expression of nitroreductase from an introduced gene can increase their sensitivity to CB1954 by over

1000-fold (5). This forms the basis of a gene-directed enzyme prodrug therapy (GDEPT) approach to cancer gene therapy (6, 7). The cell cycle independent action of the NfsB/CB1954 combination may have advantages over other enzyme/prodrug systems for cancer gene therapy such as thymidine kinase/ganciclovir and cytosine deaminase/5-fluorocytosine that target only dividing cells (8).

One limiting factor in the use of the NfsB/ CB1954 combination is the low affinity of nitroreductase for the prodrug substrate and the low reaction rate (9, 10). The enzyme has a broad substrate range and is ~10-fold more reactive with the antibiotic nitrofurazone (Scheme 1C) and ~100-fold more reactive with the quinone, menadione (Scheme 1D). The natural substrate is unknown, but expression of NfsB is induced by oxidative stress, suggesting it may be involved in detoxification reactions (11). In previous work we made a series of single mutations around the active site of NfsB, based on our crystal structure of the protein (12), and assayed the mutants *in vivo* for killing bacterial cells in the presence of CB1954 (10). We found that a number of these mutations increase the activity of the enzyme for the prodrug, the most active being F124N, where at residue 124 phenylalanine is replaced by asparagine. In a previous paper we showed that purified enzymes with single mutations at six different positions are also more active *in vitro* and show enhanced selectivity for CB1954 over nitrofurazone (13). We also showed that a double mutant, N71S/F124K combines the

[†]D.J. was supported by a BBSRC CASE studentship (to E.I.H. and S.A.W.) with ML Laboratories, M.J. was supported by a studentship from the Iranian Ministry for Health and Medical Education, and C.P.G. was funded by MRC UK Cooperative Group Component Grant G0000252 (to P.F.S.).

*To whom correspondence should be addressed. Tel: 44 (0) 121-414-5393. Fax: 44 (0) 121-414-5925. E-mail: e.i.hyde@bham.ac.uk.

Abbreviations: CB1954, 5-(aziridin-1-yl)-2,4-dinitrobenzamide; GDEPT, gene-directed enzyme prodrug therapy; NFZ, nitrofurazone.

activities of two single mutations and is more active than F124N *in vitro*. This led us to combine several other favorable single mutations to give a series of double mutants, which we have tested in a bacterial cell assay (M. Jaberipour and P. F. Searle, submitted). The most active of these double mutants is T41L/N71S. More recently, we have used a phage selection system to select NfsB mutants that induce the SOS response in bacteria when challenged with low concentrations of CB1954 (14). This enabled us to select mutants from a large λ bacteriophage library containing combinations of up to three mutations. We found several mutants that are more active than F124N in this assay, the most active being the triple mutant T41Q/N71S/F124T (14). Figure 1 shows the structure of the active site of the wild-type protein complexed to the inhibitor nicotinic acid (12) and the positions of the mutations studied. In this paper we present a full steady-state and stopped-flow kinetic characterization of the reduction of CB1954 and nitrofurazone by our most active single, double, and triple mutants and compare this with wild-type NfsB. Our most active enzyme shows ~ 100 -fold greater specificity constant with CB1954 but similar activity with nitrofurazone to the wild-type enzyme, leading to a reversal in substrate preference between the two nitroaromatic substrates. This mutant is also regioselective for the 4-nitro group of CB1954, thus generating the more cytotoxic product.

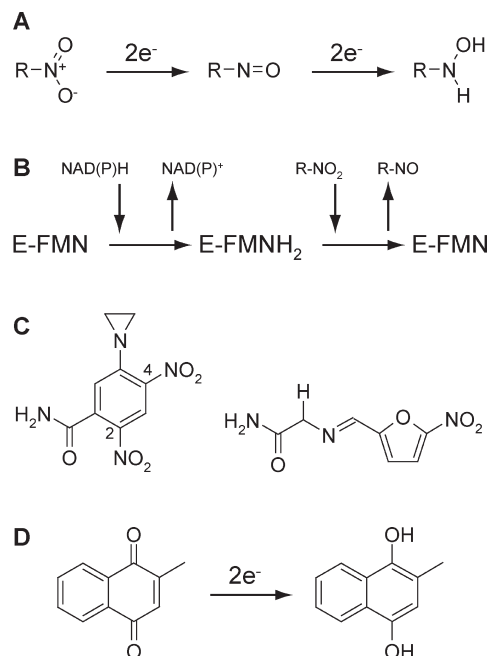
EXPERIMENTAL PROCEDURES

Protein Preparation. Wild-type NfsB was expressed from *E. coli* BL21(λ DE3) transformed with a pET11c plasmid derivative containing the *nfsB* gene, as described previously (12). The mutant proteins were expressed from *E. coli* UT5600 (*nfsB*[−]) lysogens containing single copies of the λ prophage vector λ JG3J1 carrying the *nfsB* gene, generated as described previously (10). Construction of the F124N mutation (10) and the triple T41Q/N71S/F124T mutation (14) was described previously. The double mutant T41L/N71S was made by combination of the two single mutations, using overlapping PCR fragments, analogously to the N71S/F124K enzyme described previously (13). The proteins were purified using chromatography on phenyl-Sepharose and Q-Sepharose columns as described previously (9, 12) and were $>90\%$ pure based on Coomassie-stained gels. Protein concentrations were determined by Bradford assays, calibrated against bovine serum albumin (15), or by using a molar absorbance of $43000 \text{ M}^{-1} \text{ cm}^{-1}$ at 280 nm, estimated from its amino acid composition and FMN content (16). To check that the purified proteins were saturated with FMN, the ratio of absorbance at 280 nm to that at 454 nm was measured.

Steady-State Kinetic Studies. All steady-state enzyme kinetics experiments were monitored spectrophotometrically as described previously (17). Reactions were performed in 10 mM Tris-HCl, pH 7.0, and 4.5% DMSO at 25 °C, and initiated by addition of a small volume of enzyme (final concentration $\sim 10 \text{ nM}$). All substrates were dissolved in 90% DMSO and 10% 100 mM Tris-HCl, pH 7.0. Substrate concentration ranges were 0–1 mM NADH, 0–4.5 mM CB1954, 0–2.5 mM NFZ, and 0–1.6 mM menadione, estimated either from their molar absorbances ($\epsilon_{420} = 6220 \text{ M}^{-1} \text{ cm}^{-1}$ for NADH (18), $\epsilon_{327} = 11600 \text{ M}^{-1} \text{ cm}^{-1}$ for CB1954 (19), $\epsilon_{400} = 12960 \text{ M}^{-1} \text{ cm}^{-1}$ for NFZ (20)) or by weight.

For CB1954, the initial rate of formation of the 2- and 4-hydroxylamine reduction products was monitored at 420 nm. At this wavelength both reduction products have the same molar

Scheme 1: Reactions Catalyzed by NfsB and Some of Its Substrates: (A) Reduction of Nitro Groups to Hydroxylamines, (B) the Substituted Enzyme Mechanism, (C) Structure of CB1954 (Left) and Nitrofurazone (Right), and (D) Reduction of Menadione



absorbance ($1200 \text{ M}^{-1} \text{ cm}^{-1}$). For nitrofurazone, the initial rate of disappearance of nitrofurazone was monitored, either at 420 nm, using $\Delta\epsilon_{420} = 4300 \text{ M}^{-1} \text{ cm}^{-1}$, or at 440 nm, using $\Delta\epsilon_{440} = 880 \text{ M}^{-1} \text{ cm}^{-1}$. To monitor menadione reduction, a coupled reaction was used. The assay mixture contained $100 \mu\text{M}$ cytochrome *c*, in addition to the other reagents, and the reduction of cytochrome *c* by the reduced menadione was measured using $\Delta\epsilon_{550\text{nm}} = 21100 \text{ M}^{-1} \text{ cm}^{-1}$. This enhanced the sensitivity of the assay and allowed measurements at low menadione concentrations without substrate depletion. The rates obtained were divided by 2 as menadione reduces 2 equiv of cytochrome *c*. Control reactions showed that, under these conditions, the rates measured in the presence of cytochrome *c* were the same as in its absence.

Analysis of kinetic data was performed using nonlinear regression with equal weighting of the points using Sigmaplot (SPSS, U.K.). In all cases, initial rates were measured with one substrate held at a fixed concentration and varying the other substrate, A. These rates v_i were fitted to a simple Michaelis–Menten equation:

$$\frac{v_i}{[E]} = \frac{k_{\text{catapp}}[A]}{K_{\text{mAapp}} + [A]} \quad (1)$$

where [E] is the concentration of enzyme, [A] is the concentration of the variable substrate, k_{catapp} is the apparent k_{cat} , and K_{mAapp} is the apparent K_{m} for substrate A at that concentration of substrate B.

NfsB follows a bi-bi substituted enzyme mechanism (Scheme 1B) where the bound FMN cofactor is initially reduced by NAD(P)H, releasing NAD(P)⁺, and then the reduced enzyme reacts with the nitroaromatic or quinone substrate. (9, 17, 21). To obtain the global kinetic parameters, kinetic measurements were taken over a range of concentrations of each substrate and fitted to eq 2, which describes the overall “ping-pong”

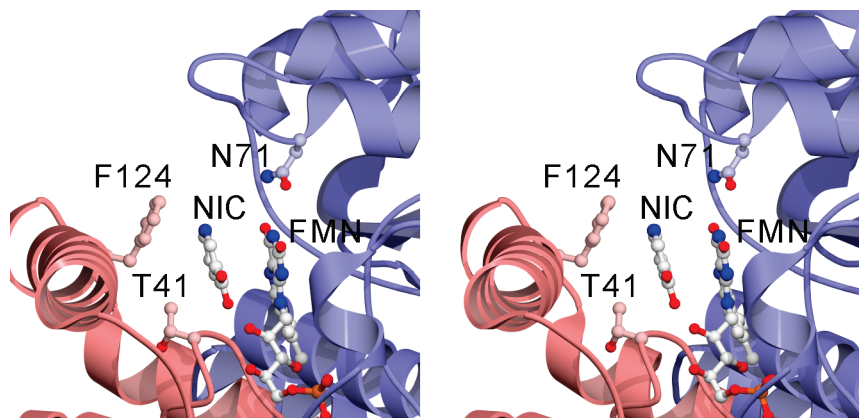


FIGURE 1: Stereo representation of the structure of the active site of wild-type nitroreductase NfsB in complex with nicotinic acid (12) and the positions of the mutations in this study. The backbone of the enzyme is shown as a ribbon with the two subunits of the enzyme in red and blue, respectively. The FMN cofactor, nicotinic acid (NIC), and side chains of F124, T41, and N71 are shown as ball and sticks. The enzyme is a homodimer; both active sites are equivalent and contain residues from each subunit. The figure was prepared using PovRay and Molscript (32).

reaction (22):

$$\frac{v_i}{[E]} = \frac{k_{\text{cat}}[A][B]}{K_{\text{mA}}[B] + K_{\text{mB}}[A] + [A][B]} \quad (2)$$

where k_{cat} , K_{mA} , and K_{mB} are the values for the Michaelis constants of each substrate when the other substrate is at infinite concentration. For a bi-bi substituted enzyme reaction, k_{cat} and K_{m} each contain kinetic terms from both oxidative and reductive halves of the reaction; however, $k_{\text{cat}}/K_{\text{m}}$ is independent of the second substrate and only contains kinetic terms from one-half of the reaction.

Stopped-Flow Kinetic Measurements. Wild-type and mutant enzymes were passed over a G10 column to remove excess FMN and to exchange the buffer into 10 mM Tris-HCl, pH 7.0, and 5% DMSO and diluted to $\sim 40 \mu\text{M}$. They were reduced in an anaerobic chamber by addition of dithionite, monitoring the absorbance of the enzyme-bound FMN cofactor at 454 nm, until the solutions were almost colorless. Equal volumes of reduced enzyme and either CB1954 or nitrofurazone ($100 \mu\text{M}$ – 2 mM) were mixed in an Applied Photophysics stopped-flow spectrophotometer (SX.17MV) at 25°C , in an anaerobic cabinet, and the reactions monitored at 454 nm to observe the reoxidation of the bound FMN in a single turnover experiment. If the substrate is at a much higher concentration than the enzyme, this reaction is pseudo-first-order. The absorbance (A) of the enzyme-bound FMN cofactor with time was fitted to a single exponential to obtain a pseudo-first-order rate constant for the reductive half-reaction:

$$A = A_0 + Ce^{-kt} \quad (3)$$

where A_0 is the initial absorbance after mixing, C is the amplitude of the reaction, k is the rate constant, and t is the time after mixing. The rate constants were plotted against substrate concentration and fitted either to a straight line or to a hyperbola (eq 1). The latter is analogous to the Michaelis–Menten equation for this half-reaction alone (23).

Analysis of CB1954 Reaction Regiospecificity. A reaction mixture containing $200 \mu\text{M}$ CB1954, 1 mM NADH, and $1 \mu\text{M}$ NfsB in 10 mM Tris-HCl, pH 7.0, and 4.5% DMSO was incubated for 5 min. The products from $20 \mu\text{L}$ of reaction were separated by semipreparative reverse-phase HPLC, using a Technicol C18 reverse-phase column ($50 \times 220 \text{ mm}$) with a 5–50% acetonitrile gradient over 25 min. All reactants were kept

anaerobic by degassing of solutions prior to reaction and sparging with helium during incubation of the reaction mixture and separation. Products were identified by their absorbance measured simultaneously at four different wavelengths (246, 260, 310, and 397 nm), each at or close to absorbance maxima for one or more product. The amount of 2- and 4-hydroxylamine product isolated using this system was determined using $\epsilon_{260\text{nm}} = 7880 \text{ M}^{-1} \text{ cm}^{-1}$ for the 4-hydroxylamine and $\epsilon_{260\text{nm}} = 5420 \text{ M}^{-1} \text{ cm}^{-1}$ for the 2-hydroxylamine (24).

RESULTS

Steady-State Data. We have previously isolated mutants of NfsB that enhance the sensitivity of *E. coli* cells to CB1954. To examine the molecular effects of these mutations, we have here purified the most active single, double, and triple mutants as well as the wild-type enzyme and determined their steady-state kinetic parameters with CB1954. Figure 2a shows the rates of reduction of different concentrations of CB1954 in the presence of $500 \mu\text{M}$ NADH by the selected enzymes. All of the data have been fitted to the simple Michaelis–Menten equation (eq 1). At this concentration of NADH both the wild-type enzyme and the F124N single mutant show very high apparent K_{m} values for CB1954. For these enzymes, it is only possible to obtain the initial, almost linear, part of the Michaelis–Menten curve, due to the limited solubility of CB1954. This gives a good estimate of the specificity constant, $k_{\text{cat}}/K_{\text{m}}$, for these enzymes but poor estimates of apparent k_{cat} or apparent K_{m} individually. The triple mutant (T41Q/N71S/F124T) shows a full Michaelis–Menten curve, with a much lower apparent K_{m} and higher apparent k_{cat} than the wild-type protein, while the double mutant (T41L/N71S) has the lowest apparent K_{m} for CB1954 and a slightly lower apparent k_{cat} than the triple mutant.

To determine the full kinetic parameters for CB1954 reduction, the steady-state kinetic experiments were repeated at a series of NADH and CB1954 concentrations. Figure 2b shows a 3D plot of all the kinetic data for reduction of CB1954 by the triple mutant fitted to the full equation for a bi-bi substituted enzyme reaction mechanism (eq 2). This allows the estimation of the values for k_{cat} , K_{mCB1954} , and K_{mNADH} at saturation by each substrate (Table 1). Because the K_{m} values for CB1954 for the wild-type and F124N mutant are much higher than the concentration of prodrug achievable in solution, the kinetic parameters for these enzymes are defined less precisely than for the double

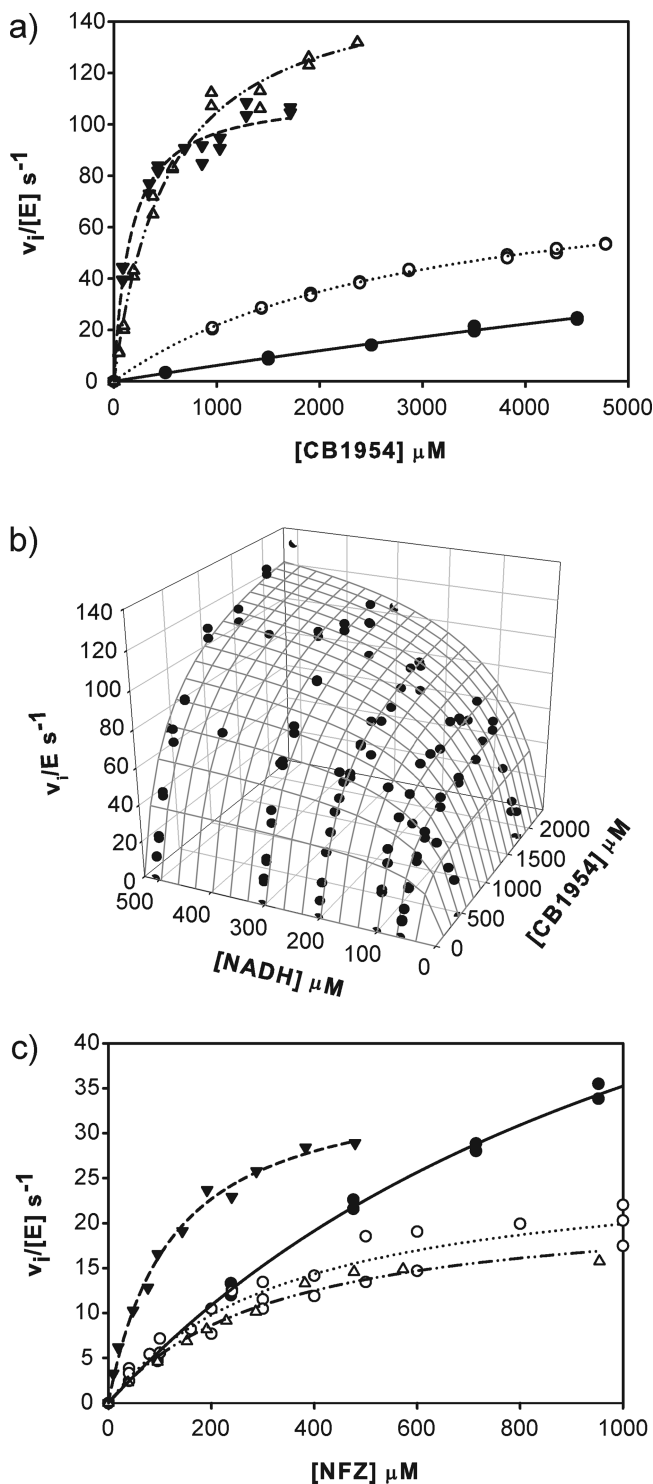


FIGURE 2: Steady-state kinetic data of the nitroreductase-catalyzed reduction of (a, b) CB1954 and (c) nitrofurazone by NADH. (a) Plots of initial rate ($v_i/[E]$) vs CB1954 concentration at 500 μM NADH for wild-type NfsB (black circles, solid lines), F124N (white circles, dotted lines), T41L/N71S (black triangles, dashed lines), and T41Q/N71S/F124T (white triangles, dotted and dashed lines). The symbols show the data while the lines show the fits to eq 1. (b) 3D plot of initial rate $v_i/[E]$ vs CB1954 and NADH concentrations for the triple mutant. The symbols show the data, while the mesh shows the fit to eq 2 using the parameters in Table 1. (c) Plots of initial rate ($v_i/[E]$) vs nitrofurazone concentration at 200 μM NADH for wild-type and mutant nitroreductase enzymes, labeled as in panel a.

and triple mutant. However, the specificity constant, k_{cat}/K_m , for CB1954 is well-defined for all of the enzymes. The specificity

constant for CB1954 for the F124N mutant is about 4-fold higher than that for the wild-type enzyme, in agreement with our previous study at a single NADH concentration (13). The triple mutant shows a specificity constant about 40-fold higher than the wild-type protein while the double mutant has the highest specificity constant, 100-fold higher than the wild-type enzyme. While the specificity constant of each of the mutants for CB1954 varies widely, the estimated k_{cat} for all of the proteins differ at most by a factor of 2.

To examine the substrate specificity of the enzymes, similar steady-state kinetic experiments were done with nitrofurazone as the substrate, instead of CB1954. Figure 2c shows the data at 200 μM NADH. In contrast to CB1954, the specificity constants for the triple mutant and F124 enzymes with nitrofurazone are similar to that for the wild-type enzyme, while that for the double mutant is only 2-fold higher than that of the wild type. The global parameters obtained for the reduction of nitrofurazone (Table 2) suggest that for F124N and the triple mutant both k_{cat} and K_m are about half of those for the wild-type enzyme, leading to similar specificity constants for all three enzymes. For T41L/N71S the K_m for nitrofurazone is approximately 7-fold lower than for the wild-type enzyme; however the k_{cat} is also lower, so overall the specificity constant is only a factor of 2 higher.

For menadione, kinetic assays were measured solely at 500 μM NADH in order to determine the specificity constants (Table 3, Supporting Information Figure 1). For this reaction, F124N and the triple mutant have specificity constants ~ 4 -fold and ~ 27 -fold higher than the wild-type enzyme, respectively, with small effects on k_{cat} . The double mutant again has lower apparent k_{cat} than the wild type, but an extremely low apparent K_m leading to a specificity constant for this enzyme ~ 30 -fold higher than the wild-type enzyme.

Stopped-Flow Kinetics. Nitroreductase shows bi-bi substituted enzyme kinetics, whereby the flavin cofactor (which is tightly bound to the enzyme) is initially reduced by NAD(P)H and, in a second step, the nitroaromatic substrate is reduced (Scheme 1B) (9, 17, 21). To elucidate further the effect of the mutations, stopped-flow kinetic measurements were taken of the reduction of CB1954 by reduced enzymes. The FMN cofactor bound to wild-type and mutant enzymes was reduced in an anaerobic chamber by addition of dithionite, followed by removal of the excess dithionite using a gel filtration column. The enzymes were then reacted with differing concentrations of CB1954 and the reactions monitored by observing the oxidation of the bound cofactor, using a stopped-flow spectrophotometer. As expected, the reactions showed pseudo-first-order kinetics (Supporting Information Figure 2). Figure 3a shows the plots of the first-order rate constants as a function of CB1954 concentration for the wild-type enzyme and the different mutants. For all of the enzymes the plots show only the initial, almost linear part, of the expected hyperbola, showing that these concentrations are well below saturation of the enzyme by CB1954. For the wild-type protein and the F124N protein, it was not possible to increase the CB1954 concentration due to its insolubility. In contrast, for the double and triple mutants it was not possible to obtain data at higher CB1954 concentrations as the reaction was nearly complete in the dead time of the instrument. Hence for all of the enzymes it is only possible to obtain the initial slopes of the plots, giving the second-order rate constant k_1/K_d for this step, not the individual values of the maximum rate constant for the reduction of CB1954 (k_1) nor its dissociation constant, K_d . The second-order rate constants obtained from this plot for all of

Table 1: Kinetic Parameters for Reduction of CB1954 by Wild-Type and Mutant NfsB^a

protein	k_{cat} (s ⁻¹)	K_{mCB1954} (μM)	$k_{\text{cat}}/K_{\text{mCB1954}}$ (μM ⁻¹ s ⁻¹)	K_{mNADH} (μM)	$k_{\text{cat}}/K_{\text{mNADH}}$ (μM ⁻¹ s ⁻¹)
wild type	140 ± 32	17200 ± 4800	0.007 ± 0.0006	40 ± 12	3.46 ± 0.6
F124N	95 ± 7	3080 ± 465	0.031 ± 0.006	55 ± 7	1.73 ± 0.018
T41L/N71S	153 ± 8	216 ± 33	0.71 ± 0.08	253 ± 41	0.62 ± 0.08
T41Q/N71S/F124T	181 ± 7	569 ± 45	0.318 ± 0.016	136 ± 12	1.33 ± 0.077

^a Initial rates were monitored at 420 nm at a series of CB1954 and NADH concentrations and fitted to the full Michaelis–Menten equation for a bi-bi substituted enzyme mechanism (eq 2) using nonlinear regression in Sigma Plot, with equal weighting of points. Errors shown are those for the fits to the equation.

Table 2: Kinetic Parameters for Reduction of Nitrofurazone by Wild-Type and Mutant NfsB^a

protein	k_{cat} (s ⁻¹)	K_{mNFZ} (μM)	$k_{\text{cat}}/K_{\text{mNFZ}}$ (μM ⁻¹ s ⁻¹)	K_{mNADH} (μM)	$k_{\text{cat}}/K_{\text{mNADH}}$ (μM ⁻¹ s ⁻¹)
wild type ^b	225 ± 34	1850 ± 400	0.15 ± 0.02	350 ± 75	0.64 ± 0.17
F124N	110 ± 12	972 ± 208	0.11 ± 0.01	315 ± 59	0.35 ± 0.05
T41L/N71S	103 ± 8	237 ± 39	0.38 ± 0.03	343 ± 51	0.30 ± 0.03
T41Q/N71S/F124T	142 ± 21	1040 ± 261	0.137 ± 0.02	347 ± 96	0.41 ± 0.07

^a Initial rates were monitored at 420 or 440 nm at a series of nitrofurazone and NADH concentrations and fitted to the full Michaelis–Menten equation for a bi-bi substituted enzyme mechanism (eq 2) using nonlinear regression in Sigma Plot, with equal weighting of points. Errors shown are those for the fits to the equation. ^b From Race et al. (17).

Table 3: Kinetic Parameters for Reduction of Menadione by Wild-Type and Mutant NfsB at 500 μM NADH^a

protein	k_{catapp} (s ⁻¹)	K_{mapp} (μM)	$k_{\text{cat}}/K_{\text{m}}$ (μM ⁻¹ s ⁻¹)
wild type	103 ± 3	150 ± 15	0.69 ± 0.05
F124N	73.7 ± 5.0	24.3 ± 6.3	3.0 ± 0.6
T41L/N71S	42.5 ± 2.4	2.0 ± 0.4	21.0 ± 3.7
T41Q/N71S/F124T	138 ± 6	7.3 ± 1.4	18.8 ± 3

^a Initial rates were monitored at 550 nm, via the coupled reduction of cytochrome *c*, at a series of menadione concentrations and fitted to the simple Michaelis–Menten equation (eq 1) using nonlinear regression in Sigma Plot, with equal weighting of points. Errors shown are those for the fits to the equation.

the enzymes are given in Table 4. As expected, the effects of the mutations on k_1/K_d are similar to those on the steady-state specificity constants, $k_{\text{cat}}/K_{\text{m}}$. For a simple substituted enzyme reaction these parameters contain the same elementary rate constants. The double mutant is about twice as active as the triple mutant, and both of these are much more active than the single mutant and the wild-type protein.

Similar stopped-flow experiments were also done with nitrofurazone as the substrate for the reduced enzyme. Again, linear plots of first-order rate constant vs nitrofurazone concentration were obtained (Figure 3b), but the second-order rate constants of the mutants vary much less than those for CB1954. The F124N mutant shows ~2-fold lower activity than the wild-type protein while the double mutant shows ~2-fold enhanced activity over the wild type and triple mutant (Table 4). For menadione as substrate with the wild-type enzyme, the reaction was complete within the dead time of the instrument, and so the rate constants could not be measured.

Regiospecificity of Reaction with CB1954. The lack of selectivity of NfsB for the two nitro groups of CB1954 results in only 50% yield of the more cytotoxic 4-hydroxylamine product, with 50% of the 2-hydroxylamine derivative. In our studies of single mutants we have shown that while most mutants show a similar lack of selectivity as the wild type, the T41L mutant tips the product ratio 3:1 in favor of the more cytotoxic derivative (13). To determine the selectivity of the double and triple

mutants in this study, the products of CB1954 reduction were separated by HPLC and monitored at four different wavelengths to determine their identity. Figure 4 shows the HPLC traces of the reaction products of the wild-type enzyme and the T41L/N71S mutant with CB1954. For the double mutant, the predominant product was the 4-hydroxylamine, with negligible amounts of the 2-hydroxylamine; however, the triple mutant T41Q/N71S/F124T showed no selectivity for either of the two nitro groups (data not shown).

DISCUSSION

We have examined the kinetics of wild-type NfsB and three NfsB mutants with CB1954, nitrofurazone, and menadione. For the wild-type protein, our estimates of the global k_{cat} and K_{m} for CB1954 are about 20-fold higher than those reported by Anlezark et al. (9). However, the specificity constant, $k_{\text{cat}}/K_{\text{m}}$, which is the key parameter determining the rate of reaction at low substrate concentrations, agrees with that determined previously (9). We previously found a similar (approximately 20-fold) discrepancy between the global kinetic values of the Michaelis constants for nitrofurazone for the wild-type enzyme determined by Anlezark, using a stopped assay, and by our group, using a continuous spectroscopic method (17). We attribute the differences between the estimates as due to substrate depletion at the high enzyme concentrations and long times used in the stopped assays. The low specificity constant for CB1954 found in both studies shows that the prodrug is a poor substrate for the wild-type enzyme. The ~4-fold increased specificity constant of the F124N mutant for CB1954 over the wild-type enzyme is in agreement with our previous study at 60 μM NADH (13). By determining the global kinetic parameters, we show here that there is little difference in k_{cat} for CB1954 between the two enzymes. This study further shows that the double and triple mutants isolated have much greater increases (50–100-fold) in specificity constant for CB1954 over the wild-type NfsB, again with little effect in k_{cat} for the prodrug.

In contrast, there is much less variation in specificity constants between the wild-type enzyme and the mutants with the antibiotic nitrofurazone, the greatest effect being an ~2-fold increase for the double mutant. This leads to reversed substrate selectivity in

the most active mutants. Whereas the wild-type enzyme has a 20-fold higher specificity constant for nitrofurazone than CB1954, the double and triple mutants have ~2-fold greater specificity constant for CB1954, the triple mutant showing slightly greater selectivity than the double mutant (Table 4). As in our study of the single mutants, we attribute this difference in the effects of the mutations to the different steric requirements of the two nitroaromatic substrates. CB1954 is a six-membered ring with four side chains around it, and so steric effects at the active site of the enzyme may affect binding of this substrate more than that of nitrofurazone, a five-membered ring with a single, long

side chain. This interpretation is supported by the effect of the mutations on the reduction of menadione. Menadione contains two fused 6-membered rings, and the mutations affect the specificity constants for reduction of this substrate in a similar way, but to a slightly lesser extent, to their effect on CB1954.

The effects of the mutations seen in the steady-state measurements of specificity constants k_{cat}/K_m are mirrored in the stopped-flow measurements of the second-order rate constant, k_1/K_d , confirming the effects. In addition, the isolation of the reduced enzyme and its reactivity with the substrates in the stopped-flow assays prove conclusively that the reaction goes via a substituted enzyme mechanism, as expected from steady-state kinetic measurements (9, 17, 21). Although we obtained estimates of the second-order rate constant, we were not able to measure the dissociation constants K_d for CB1954 or nitrofurazone, nor the rate constants for reduction of these substrates at saturation. However, the highest rates of FMN oxidation observed in the stopped-flow assays for the double and triple mutants for CB1954 (350–550 s^{-1}) and for the double mutant with nitrofurazone (500 s^{-1}) are much higher than the global steady-state rate constants for the reactions (100–200 s^{-1}). This shows that the steady-state rates for these reactions are determined by a step other than the chemical reduction observed in the stopped-flow reaction. For wild-type enzyme we have also measured the rate of reduction of FMN by NADH. Here again, the maximum rate measured was limited by the dead time of the stopped-flow instrument ($> 500 \text{ s}^{-1}$), much faster than the steady-state rate of the reactions (data not shown). Interestingly, the global steady-state rate constants for all four enzymes with both CB1954 and nitrofurazone are similar. We suggest that for all of the reactions the rate is likely to be limited by product release (either NAD^+ or nitroso aromatic) occurring at the global steady-state rate measured, $\sim 150 \text{ s}^{-1}$, for all of the enzymes. This rate may be limited

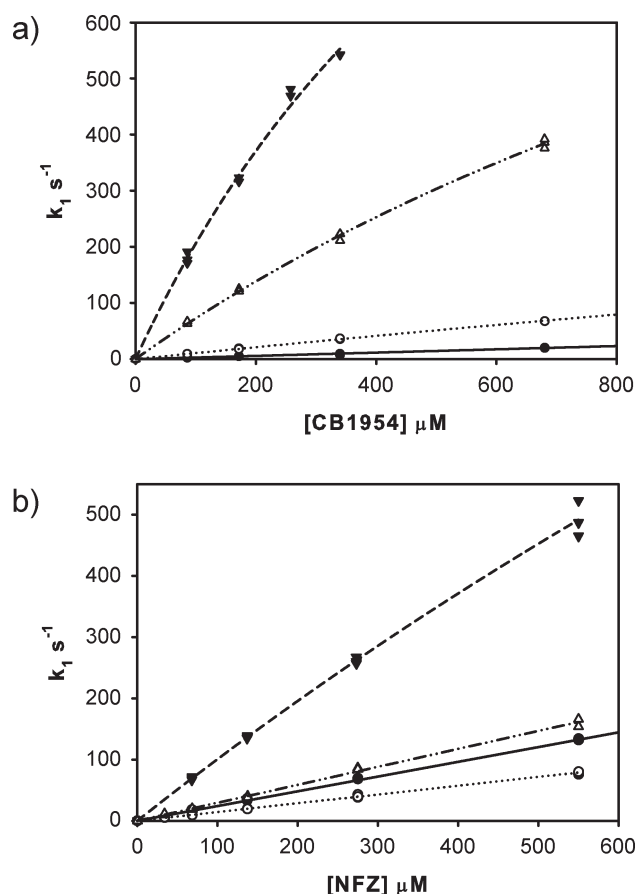


FIGURE 3: Stopped-flow kinetic assays of the reduction of CB1954 and nitrofurazone by reduced wild-type and mutant nitroreductase enzymes. (a) Plots of the apparent first-order rate constants vs CB1954 concentration for wild-type and mutant enzymes: wild-type NfsB (black circles, solid lines), F124N (white circles, dotted lines), T41L/N71S (black triangles, dashed lines), and T41Q/N71S/F124T (white triangles, dotted and dashed lines). Symbols show the measured rates with lines showing the fits, either to a straight line or to eq 1. (b) Plots of the apparent first-order rate constants vs nitrofurazone concentration for wild-type and mutant enzymes, labeled as in (a).

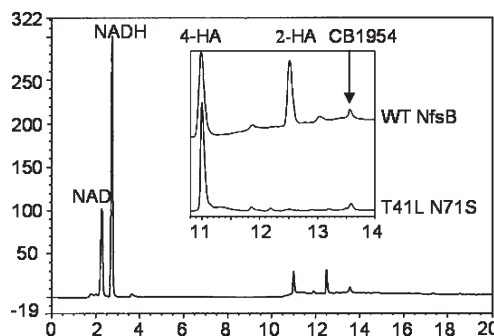


FIGURE 4: HPLC chromatogram of the reaction products of nitroreductase with CB1954 and NADH monitored at 246 nm. Main trace: Products and reactants from reaction with the wild-type enzyme. Inset: Comparison of products following incubation with wild-type NfsB (upper trace) and the T41L/N71S enzyme (lower trace).

Table 4: Apparent Second-Order Rate Constants (k_1/K_d) for the Reoxidation of Wild-Type and Mutant Nitroreductase Enzymes with CB1954 or Nitrofurazone^a

protein	k_1/K_d for CB1954 (a) ($\mu\text{M}^{-1} \text{ s}^{-1}$)	k_1/K_d for nitrofurazone (b) ($\mu\text{M}^{-1} \text{ s}^{-1}$)	selectivity for CB1954 over nitrofurazone, ratio a/b
wild type	0.029 ± 0.001	0.38 ± 0.06	0.076
F124N	0.108 ± 0.002	0.165 ± 0.007	0.65
T41L/N71S	1.6 ± 0.1	0.9 ± 0.1	1.77
T41Q/N71S/F124T	0.76 ± 0.02	0.39 ± 0.04	1.95

^a The first-order rate constants were fitted either to a linear equation or to a hyperbola (eq 1) using nonlinear regression in Sigma Plot, with equal weighting of the points. Errors shown are those for the fits to the equations.

by a conformational change as seen in a number of enzymes including *E. coli* dihydrofolate reductase (reviewed in ref 25).

The effects of the mutations are unlikely to be due to conformational changes as, in our previous study, we showed that the single mutations T41L, F124N, and F124K affect the protein primarily only at the mutated amino acid, with minimal changes elsewhere. The N71S mutation replaces a direct hydrogen bond from the asparagine side chain to the FMN cofactor by one from a solvent water molecule, hydrogen bonded to the serine, while the double mutant N71S/F124K combines the structural changes seen for each of the single mutations (13). The effects of the mutations are therefore likely to be either steric or due to changes in polarity at the active site. In addition to its enhanced activity with CB1954, the T41L/N71S mutant, like the T41L mutant (13), shows greater regioselectivity for the 4-nitro group of the substrate. This regioselectivity is not seen for the T41Q/N71S/F124T triple mutant, suggesting that this discrimination is likely to be due to the hydrophobicity of the leucine side chain at position 41. A recent computational study suggests that the mechanism of reduction of CB1954 by NfsB is by electron transfer from FMN to the nitroaromatic ring, followed by protonation from solvent (26). This implies that the product distribution depends on the solvent accessibility of the two nitro groups. In addition, the backbone NH group of T41 may hydrogen bond to the amide group of CB1954. In the T41L mutants the backbone NH remains; however, the leucine side chain could either affect the orientation of CB1954 or, alternatively, affect the solvent distribution at the active site of the enzyme so changing protonation of the product.

The 50–100-fold enhancement in specificity constant for the prodrug CB1954, seen with the double and triple mutants in this study, contrasts with mutational experiments optimizing thymidine kinase or cytosine deaminase for their prodrugs (27, 28). For these enzymes the mutants selected had reductions of 20–200-fold in specificity constant for their natural substrates, thymine and cytosine, respectively, with little improvement (maximum 2–5-fold) in the specificity constants for the prodrugs. The major effect of these mutations is therefore to reduce competition from the natural substrates *in vivo*. In this study, the increase in specificity constant for CB1954 of the double and triple mutants makes these mutants much more effective catalysts for reduction of the prodrug.

As the concentration of CB1954 achievable in patients is very low ($\sim 10 \mu\text{M}$) (29), much lower than its K_m , the rate of reaction should be proportional to the specificity constant of the enzyme. Hence the double and triple mutant enzymes should be much more reactive than wild-type NfsB, *in vivo*. While the 4-hydroxylamine derivative of CB1954 is more cytotoxic than the 2-hydroxylamine product (30), the latter shows a greater bystander effect, killing neighboring cells that do not express the enzyme (31). This is important for GDEPT as not all tumor cells will be infected with the viral vector containing the gene for the prodrug-activating enzyme. Therefore, both of these mutant enzymes are of potential interest for GDEPT with CB1954 while the double mutant may be of interest for selective cell ablation.

ACKNOWLEDGMENT

We thank G. Burns, School of Chemistry, University of Birmingham, for help with the HPLC analyses.

SUPPORTING INFORMATION AVAILABLE

Two figures showing (1) the steady-state kinetic data of the rate of reaction vs menadione concentration at 500 μM NADH by the four nitroreductase enzymes and (2) the stopped-flow kinetic data of absorbance of bound FMN vs time at different concentrations of CB1954 for reduced F124N nitroreductase. This material is available free of charge via the Internet at <http://pubs.acs.org>.

REFERENCES

- Roldan, M. D.; Perez-Reinado, E.; Castillo, F.; and Moreno-Vivian, C. (2008) Reduction of polynitroaromatic compounds: the bacterial nitroreductases. *FEMS Microbiol. Rev.* 32, 474–500.
- Patel, P.; Young, J. G.; Mautner, V.; Ashdown, D.; Bonney, S.; Pineda, R. G.; Collins, S. I.; Searle, P. F.; Hull, D.; Peers, E.; Chester, J.; Wallace, D. M.; Doherty, A.; Leung, H.; Young, L. S.; and James, N. D. (2009) A phase I/II clinical trial in localized prostate cancer of an adenovirus expressing nitroreductase with CB1954. *Mol. Ther.* 2009, 17, 1292–1299.
- Palmer, D. H.; Mautner, V.; Mirza, D.; Oliff, S.; Gerritsen, W.; van der Sijp, J. R.; Hubscher, S.; Reynolds, G.; Bonney, S.; Rajaratnam, R.; Hull, D.; Horne, M.; Ellis, J.; Mountain, A.; Hill, S.; Harris, P. A.; Searle, P. F.; Young, L. S.; James, N. D.; and Kerr, D. J. (2004) Virus-directed enzyme prodrug therapy: intratumoral administration of a replication-deficient adenovirus encoding nitroreductase to patients with resectable liver cancer. *J. Clin. Oncol.* 22, 1546–1552.
- Knox, R. J.; Friedlos, F.; and Roberts, J. J. (1988) The activation of CB1954 (2,4-dinitro-5-aziridinyl benzamide) in Walker cells is by bioreduction to a DNA crosslinking agent. *Br. J. Cancer* 58, 252–252.
- Weedon, S. J.; Green, N. K.; McNeish, I. A.; Gilligan, M. G.; Mautner, V.; Wrighton, C. J.; Mountain, A.; Young, L. S.; Kerr, D. J.; and Searle, P. F. (2000) Sensitisation of human carcinoma cells to the prodrug CB1954 by adenovirus vector-mediated expression of *E. coli* nitroreductase. *Int. J. Cancer* 86, 848–854.
- Grove, J. I.; Searle, P. F.; Weedon, S. J.; Green, N. K.; McNeish, I. A.; and Kerr, D. J. (1999) Virus-directed enzyme prodrug therapy using CB1954. *Anti-Cancer Drug Des.* 14, 461–472.
- Searle, P. F.; Chen, M. J.; Hu, L.; Race, P. R.; Lovering, A. L.; Grove, J. I.; Guise, C.; Jaberipour, M.; James, N. D.; Mautner, V.; Young, L. S.; Kerr, D. J.; Mountain, A.; White, S. A.; and Hyde, E. I. (2004) Nitroreductase: a prodrug-activating enzyme for cancer gene therapy. *Clin. Exp. Pharmacol. Physiol.* 31, 811–816.
- Greco, O.; and Dachs, G. U. (2001) Gene directed enzyme/prodrug therapy of cancer: historical appraisal and future perspectives. *J. Cell Physiol.* 187, 22–36.
- Anlezark, G. M.; Melton, R. G.; Sherwood, R. F.; Coles, B.; Friedlos, F.; and Knox, R. J. (1992) The bioactivation of 5-(aziridin-1-yl)-2,4-dinitrobenzamide (CB1954). I. Purification and properties of a nitroreductase enzyme from *Escherichia coli* a potential enzyme for antibody-directed enzyme prodrug therapy (ADEPT). *Biochem. Pharmacol.* 44, 2289–2295.
- Grove, J. I.; Lovering, A. L.; Guise, C.; Race, P. R.; Wrighton, C. J.; White, S. A.; Hyde, E. I.; and Searle, P. F. (2003) Generation of *Escherichia coli* nitroreductase mutants conferring improved cell sensitization to the prodrug CB1954. *Cancer Res.* 63, 5532–5537.
- Barbosa, T. M.; and Levy, S. B. (2002) Activation of the *Escherichia coli* nfnB gene by MarA through a highly divergent marbox in a class II promoter. *Mol. Microbiol.* 45, 191–202.
- Lovering, A. L.; Hyde, E. I.; Searle, P. F.; and White, S. A. (2001) The structure of *Escherichia coli* nitroreductase complexed with nicotinic acid: three crystal forms at 1.7 Å, 1.8 Å, and 2.4 Å resolution. *J. Mol. Biol.* 309, 203–213.
- Race, P. R.; Lovering, A. L.; White, S. A.; Grove, J. I.; Searle, P. F.; Wrighton, C. W.; and Hyde, E. I. (2007) Kinetic and structural characterisation of *Escherichia coli* nitroreductase mutants showing improved efficacy for the prodrug substrate CB1954. *J. Mol. Biol.* 368, 481–492.
- Guise, C. P.; Grove, J. I.; Hyde, E. I.; and Searle, P. F. (2007) Direct positive selection for improved nitroreductase variants using SOS triggering of bacteriophage lambda lytic cycle. *Gene Ther.* 14, 690–698.
- Bradford, M. M. (1976) A rapid and sensitive method for the quantitation of microgram quantities of protein utilizing the principle of protein-dye binding. *Anal. Biochem.* 72, 248–254.
- Pace, C. N.; Vajdos, F.; Fee, L.; Grimsley, G.; and Gray, T. (1995) How to measure and predict the molar absorption-coefficient of a protein. *Protein Sci.* 4, 2411–2423.

17. Race, P. R., Lovering, A. L., Green, R. M., Ossor, A., White, S. A., Searle, P. F., Wrighton, C. J., and Hyde, E. I. (2005) Structural and mechanistic studies of *Escherichia coli* nitroreductase with the anti-biotic nitrofurazone. Reversed binding orientations in different redox states of the enzyme. *J. Biol. Chem.* 280, 13256–13264.
18. Galante, Y. M., and Hatefi, Y. (1978) Resolution of complex I and isolation of NADH dehydrogenase and an iron–sulfur protein. *Methods Enzymol.* 53, 15–21.
19. Knox, R. J., Friedlos, F., Biggs, P. J., Flitter, W. D., Gaskell, M., Goddard, P., Davies, L., and Jarman, M. (1993) Identification, synthesis and properties of 5-(aziridin-1-yl)-2-nitro-4-nitrosobenzamide, a novel DNA cross-linking agent derived from CB1954. *Biochem. Pharmacol.* 46, 797–803.
20. Peterson, F. J., Mason, R. P., Hovsepian, J., and Holtzman, J. L. (1979) Oxygen-sensitive and -insensitive nitroreduction by *Escherichia coli* and rat hepatic microsomes. *J. Biol. Chem.* 254, 4009–4014.
21. Koder, R. L., and Miller, A. F. (1998) Steady-state kinetic mechanism, stereospecificity, substrate and inhibitor specificity of *Enterobacter cloacae* nitroreductase. *Biochim. Biophys. Acta* 1387, 395–405.
22. Cleland, W. W. (1963) The kinetics of enzyme-catalyzed reactions with two or more substrates or products. II. Inhibition: nomenclature and theory. *Biochim. Biophys. Acta* 67, 173–187.
23. Strickland, S., Palmer, G., and Massey, V. (1975) Determination of dissociation constants and specific rate constants of enzyme-substrate (or protein-ligand) interactions from rapid reaction kinetic data. *J. Biol. Chem.* 250, 4048–4052.
24. Knox, R. J., Friedlos, F., Marchbank, T., and Roberts, J. J. (1991) Bioactivation of CB 1954—Reaction of the active 4-hydroxylamino derivative with thioesters to form the ultimate DNA DNA interstrand cross-linking species. *Biochem. Pharmacol.* 42, 1691–1697.
25. Schnell, J. R., Dyson, H. J., and Wright, P. E. (2004) Structure, dynamics, and catalytic function of dihydrofolate reductase. *Annu. Rev. Biophys. Biomol. Struct.* 33, 119–140.
26. Christofferson, A., and Wilkie, J. (2009) Mechanism of CB1954 reduction by *Escherichia coli* nitroreductase. *Biochem. Soc. Trans.* 37, 413–418.
27. Kokoris, M. S., and Black, M. E. (2002) Characterization of herpes simplex virus type 1 thymidine kinase mutants engineered for improved ganciclovir or acyclovir activity. *Protein Sci.* 11, 2267–2272.
28. Mahan, S. D., Ireton, G. C., Knoeber, C., Stoddard, B. L., and Black, M. E. (2004) Random mutagenesis and selection of *Escherichia coli* cytosine deaminase for cancer gene therapy. *Protein Eng. Des. Sel.* 17, 625–633.
29. Chung-Faye, G., Palmer, D., Anderson, D., Clark, J., Downes, M., Baddeley, J., Hussain, S., Murray, P. I., Searle, P., Seymour, L., Harris, P. A., Ferry, D., and Kerr, D. J. (2001) Virus-directed, enzyme prodrug therapy with nitroimidazole reductase: a phase I and pharmacokinetic study of its prodrug, CB1954. *Clin. Cancer Res.* 7, 2662–2668.
30. Knox, R. J., Friedlos, F., Jarman, M., and Roberts, J. J. (1988) A new cytotoxic, DNA interstrand crosslinking agent, 5-(aziridin-1-yl)-4-hydroxylamino-2-nitrobenzamide, is formed from 5-(aziridin-1-yl)-2,4-dinitrobenzamide (CB 1954) by a nitroreductase enzyme in Walker carcinoma cells. *Biochem. Pharmacol.* 37, 4661–4669.
31. Helsby, N. A., Ferry, D. M., Patterson, A. V., Pullen, S. M., and Wilson, W. R. (2004) 2-Amino metabolites are key mediators of CB 1954 and SN 23862 bystander effects in nitroreductase GDEPT. *Br. J. Cancer* 90, 1084–1092.
32. Kraulis, P. J. (1991) MOLSCRIPT: a program to produce both detailed and schematic plots of protein structures. *J. Appl. Crystallogr.* 24, 946–950.